Engineering Structures 204 (2020) 109670

Contents lists available at ScienceDirect

Engineering Structures

journal homepage: www.elsevier.com/locate/engstruct

Numerical out-of-plane stability analysis of long span timber trusses with focus on buckling length calculations

Petr Sejkot[a,b,*], Sigurdur Ormarsson[a], Johan Vessby[c], Bo Källsner[a]

[a] Linnaeus University, P G Vejdes väg, 351 95 Växjö, Sweden
[b] Klokner Institute, Šolínova 7, 166 08 Prague, Czech Republic
[c] Karlstads University, Universitetsvägen 2, 651 88 Karlstad, Sweden

ARTICLE INFO

Keywords:
Wood
Timber truss structure
Lateral instability
Numerical simulations
Punched metal plate fasteners

ABSTRACT

According to the harmonized European design code for timber structures, Eurocode 5, all pitched timber trusses are designed as an in-plane structure, meaning that the bracing systems used are assumed to prevent the out-of-plane failure of the truss if sufficient strength and stiffness are provided. The present paper studies how the stiffness of a wooden bracing system contributes to the out-of-plane stability of a trussed roof structure. Results from numerical simulations indicate that significant bracing forces may occur in compressed structural members for long-span timber structures. As well, the values obtained from the calculations according to Eurocode 5 are occasionally far from the results obtained by numerical simulations.

1. Introduction

In Europe [1] and other regions around the world, slender timber beams connected together with punched metal plate fasteners is a common solution to form a trussed roof structure. There are various ways how to brace these structures, e.g. by use of corrugated steel sheathing or roof sheeting panels. But there are also several existing roof structures without sheathing panels on top of the top chords, typically roofs covered by roofing tiles. And such roofs with tiles and without sheathing panels are still being constructed. For stability these roofs are using bracing trusses placed in the plane of the top chords together with diagonal wind braces and roof battens, see Fig. 1. The battens are connected to bracing trusses to prevent the lateral buckling of the top chords. According to the author's opinion, these roofs might be insufficiently braced at times, because this bracing system shows a semi-rigid deformation behaviour that often results in out-of-plane buckling as a critical failure mode for the top chord design. This is especially important for long span trusses over 15 m, where metal-plate-connected timber trusses are frequently used [2,3].

In Ormarsson et al. [4], the out-of-plane buckling length was studied by using a simple 3D-beam/spring finite element model to analyse the lateral buckling behaviour of a pitched long-span timber truss structure. The 3D beam elements used to simulate the wood truss members were connected together by six independent spring elements (three for translations and three for rotations), representing the connection stiffness for each degree of freedom of the used mechanical joints. Maraghechi and Itani [5] also used this 3D-beam/spring modelling for first order static analysis of a short span timber truss structure. Compared to the commonly used design approach, which considers the connections in the roof structure to be pinned, this semi rigid approach [5] showed promising results. Burdzik and Dekker [6] adopted the semi-rigid modelling approach for three-dimensional numerical buckling analysis to simulate the whole double-W truss structure with the span of 10 meter. Their work mainly focused on how to consider the influence of the eccentricity between the centreline of the roof battens and the centreline of the compressed top chord (marked by the letter e in Fig. 1). They used beam elements to connect the centrelines of top chords and battens with cross-section and material properties that were according to Stanway et al. [7]. In contrast to Burdzik and Dekker [6], Song [8] and Pienaar [9] used full-scale tests to study the out-of-plane buckling length of the compressed top chords of the roof trusses. All of the listed studies ([6,8,9]) pointed out not negligible threat of the out-of-plane buckling for trussed roof structures stabilised by semi-rigid bracing systems in wood.

An analytical formula to calculate the out-of-plane buckling length of a top chord in a pitched long span roof truss braced with bracing trusses and diagonal wind braces (see Fig. 1) is presented by Kessel [10]:

$$l_{eff,K} = \pi \cdot \sqrt[4]{\frac{E_{0,k} I_z}{4 \cdot k}} \tag{1}$$

* Corresponding author at: Klokner Institute, Šolínova 7, 166 08 Prague, Czech Republic.
E-mail addresses: petr.sejkot@cvut.cz (P. Sejkot), sigurdur.ormarsson@lnu.se (S. Ormarsson), johan.vessby@kau.se (J. Vessby), bo.kallsner@lnu.se (B. Källsner).

https://doi.org/10.1016/j.engstruct.2019.109670
Received 5 March 2019; Received in revised form 5 September 2019; Accepted 9 September 2019
Available online 29 November 2019
0141-0296/

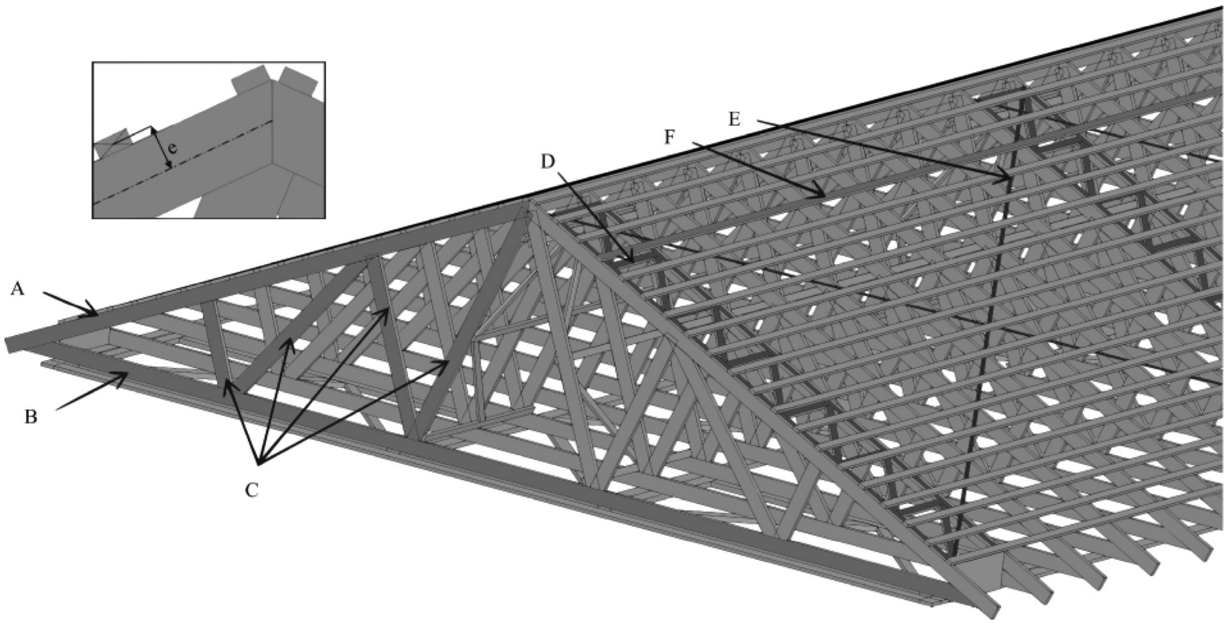

Fig. 1. Pitched timber roof structure with semi-rigid bracing system of wood: A-top chord, B-bottom chord, C-diagonals, D-bracing truss, E-wind brace, F-roof batten.

where $l_{eff,K}$ is the effective buckling length for the out-of-plane buckling of the top chord, $E_{0,k}$ is the characteristic modulus of elasticity, I_z is the moment of inertia about the weak axis of the top chord and k is the stiffness in [N/m^2] of the elastic foundation with respect to the weak axis of the top chord (i.e. a single support (spring) stiffness in [N/m] divided with the c-c distance between the battens).

Eq. (1) is based on the Timoshenko's theory [11], of a continuous beam on an elastic foundation (a so-called Winkler foundation [12]) governed by the following differential equation:

$$(EI(x)w'')'' + (N(x)w')' + k(x)w = q(x) \tag{2}$$

where E is modulus of elasticity of the beam, I is the moment of inertia of the beam, x is the length-coordinate of the beam, w is the unknown lateral deflection of the beam as a function of the x-coordinate, N is the compressive normal force, k is the stiffness of the elastic foundation of the beam, q is the lateral load acting on the beam.

In [10], Eq. (2) is applied for the top chord in the roof plane, hence the moment of inertia about the weak axis is used in Eq. (1) and the (spring) stiffness of the supports represents the stiffness of the bracing system in direction of the roof battens. Note that the displacements of the bracing trusses in the roof plane are neglected. This assumption is acceptable since the length of the half waves is small in relation to the length of the top chord, less than 1/5.

The lateral load acting on the top chord is neglected, thus the studied application is only loaded axially with a constant compressive normal force. To ensure reasonable good solution of Eq. (2), form of the first buckling mode is also assumed to consist of half waves that are at least three times the c-c distance between the roof battens (minimal length according to Timoshenko [11]). These assumptions result in a simplified differential equation usable for a top chord with a constant bracing stiffness, a constant normal force and no lateral load as

$$EI_z w^{IV} + Nw'' + kw = 0 \tag{3}$$

where I_z is the moment of inertia about the weak axis of the beam and w is the lateral deflection of the beam in direction of the battens centrelines.

By neglecting the influence of the eccentricity e shown in Fig. 1, and assuming that the top chord at its ends is simply supported and moment free (i.e. $w(0) = w(l) = 0$ and $w''(0) = w''(l) = 0$) the solution of Eq. (3) becomes

$$w(x) = A \cdot sin\frac{m\pi x}{l} \tag{4}$$

where l is the length of the beam and m is the number of half waves. After inserting Eq. (4) into Eq. (3), it can be written as

$$\left[\left(\frac{m\pi}{l}\right)^4 - \left(\frac{m\pi}{l}\right)^2\frac{N}{EI_z} + \frac{k}{EI_z}\right]A \cdot sin\frac{m\pi x}{l} = 0 \tag{5}$$

The only non-trivial solution of Eq. (5) is obtained when the term inside the brackets is equal to zero, giving the critical normal force as

$$N_{cr}(m, l) = \frac{\pi^2 E\, I_z}{l^2}\left(m^2 + \frac{kl^4}{m^2\pi^4 E\, I_z}\right) \tag{6}$$

For a fixed number of half-waves (m = 1,2,3,..), the critical normal force can be used to study the number of sinusoidal half-waves in the critical buckling shape for top chords of varying lengths, see Fig. 2.

The minimum of the critical normal force function $N_{cr,min}$ is determined by setting the partial derivative of N_{cr} with respect to l equal to zero. The obtained minimum value becomes

$$N_{cr,min} = 2 \cdot \sqrt{E \cdot I_z \cdot k} \tag{7}$$

Therefore, the minimum value depends neither on the length of the beam nor on the number of half-waves (see the diagram in Fig. 2) since it represents the critical compressive normal force of an infinitely long beam on an elastic foundation. The influence of pinned boundary conditions on the buckling modes is also shown in Fig. 2.

The length of a half-wave for a minimum of the critical normal force function $N_{cr,min}$ can be calculated as

$$l_{h-w} = \pi \cdot \sqrt[4]{\frac{E\, I_z}{k}} \tag{8}$$

According to a numerical study by Ormarsson et al. [4], Eq. (8) can be used when the minimal number of springs within a half-wave is equal to or larger than two.

Assuming that the minimum critical normal force $N_{cr,min}$ is equal to the critical compressive normal force N_{cr} of an Euler II column with the same cross section dimensions as the top chord, but without an elastic foundation, the effective buckling length is calculated with the Euler II column formula in [13] as

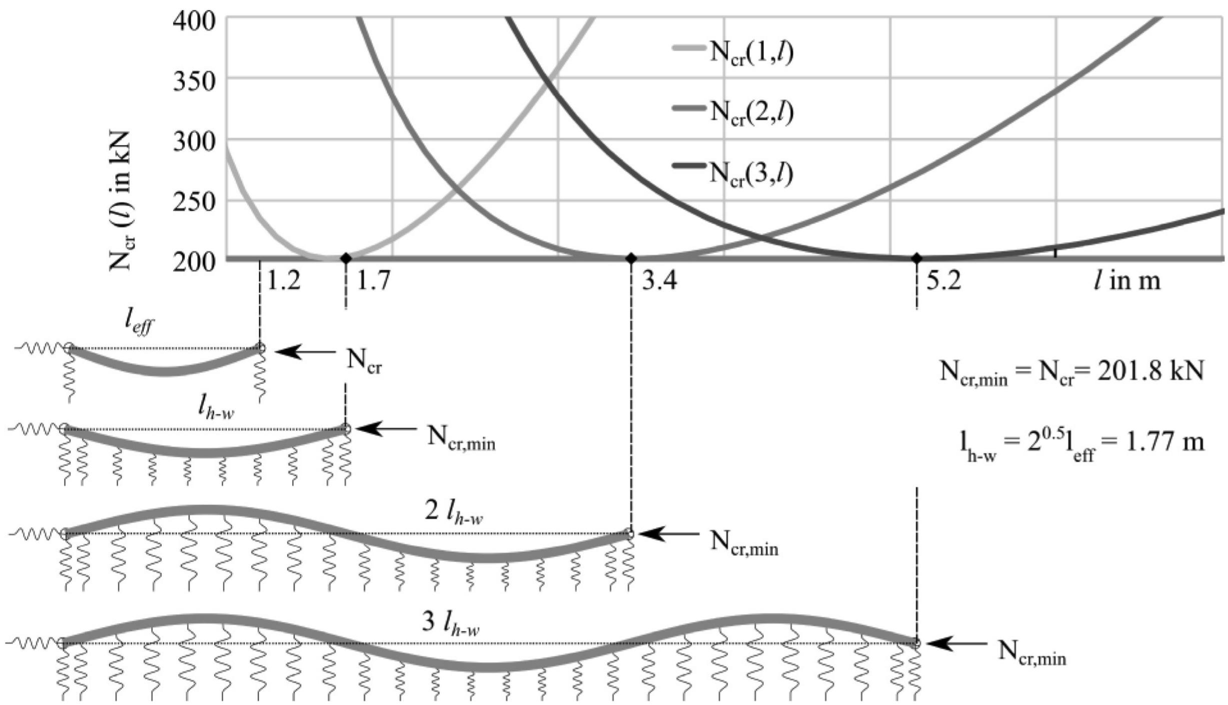

Fig. 2. Visualisation of critical normal force variation $N_{cr}(m,l)$ (according to Eq. (8) with $E_{0,k}$ = 8.461 GPa, I_z = 3.60 10^{-6} m^4, k = 335.5 kN/m^2) for one, two and three half waves.

$$l_{eff} = \sqrt{\frac{\pi^2 \cdot E_{0,k} I_z}{N_{cr}}} \tag{9}$$

To calculate the out-of-plane buckling length of a top chord, Eq. (1) can be then obtained by replacing N_{cr} in Eq. (9) with the right side of (7).

Fig. 2 shows that the numerical buckling analysis of a beam on an elastic foundation gives the same minimum critical normal force $N_{cr,min}$ as Eq. (6). By using the assumption of equality between the minimum critical normal force $N_{cr,min}$ and the critical compressive normal force N_{cr} of an Euler II column, a numerical buckling analysis can be used to find the same effective buckling length as Eq. (1), by using

$$l_{eff,z} = \frac{l_{h-w}}{\sqrt{2}} = \sqrt{\frac{\pi^2 \cdot E_{0,k} I_z}{\alpha \cdot N}} \tag{10}$$

where α is the first eigenvalue of Euler II column loaded by the reference compressive normal force N. As described above, this issue is from a purely analytical perspective, but there are reasons to choose another numerical approach.

The advantage of numerical modelling is the possibility to consider more advanced issues like:

- overall in-plane bending stiffness of the bracing truss, since it is not representing a fully stiff support;
- an efficient bracing system that provides supports to trusses in heel and crown joints;
- an orthotropic material model;
- eccentricity between the centrelines of the top chord and the bracing system;
- non-uniform normal force distribution in the top chord;
- the influence of an interaction between a compressive normal force and the biaxial bending moments on the top chord design [14];
- stabilising effect from the diagonal members connected to the top chord;
- interaction between flanges of bracing trusses and adjacent top chords;

The aim of this paper is to use the finite element method to study the behaviour of long-span pitched timber roof structure stabilised by bracing trusses in the plane of the top chord. The simulations will be used to study in detail how factors as those previously listed have influence on the top chord stability.

2. Methods

2.1. Finite element modelling

To determine the bracing system efficiency for pitched long-span trusses, a finite element simulation of the entire roof structure was performed, see Fig. 3.

The timber roof structure in Fig. 3 is simulated with quadratic 3D beam elements through a use of the finite element software Abaqus® [15]. The beams are assigned with typical material properties for wood and connected with special spring type connector elements. The result

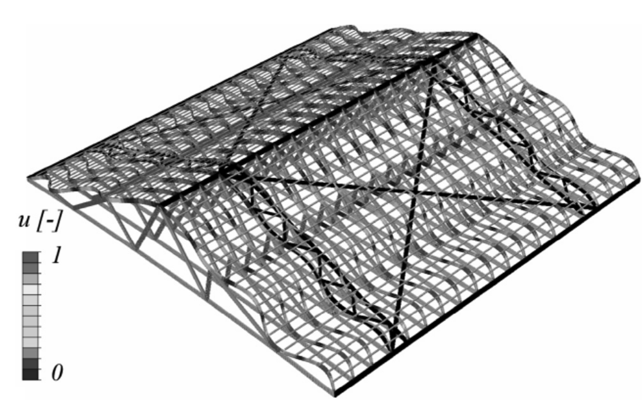

Fig. 3. Visualisation of a critical buckling mode for a roof structure loaded with a symmetric snow load as shown in Fig. 5. Colour field represents a magnitude of lateral displacement of the top chords. (For interpretation of the references to colour in this figure legend, the reader is referred to the web version of this article.)

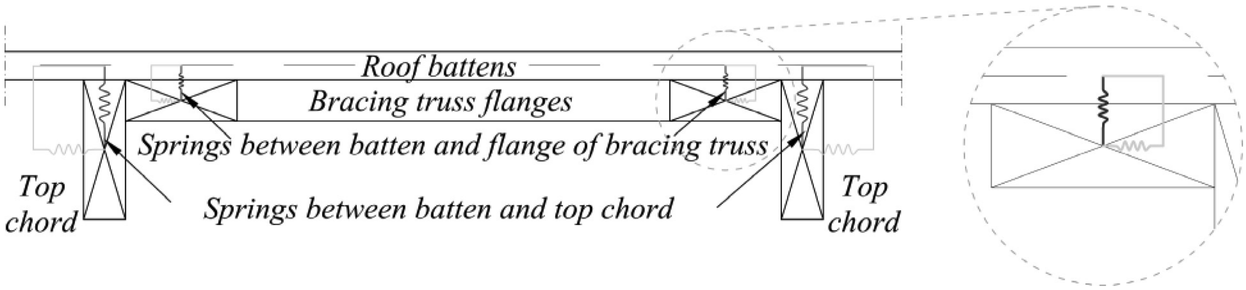

Fig. 4. Illustration of spring connections between the centre-lines of roof battens and in-plane bracing truss and adjacent top chords.

in Fig. 3 clearly shows that the maximum out-of-plane buckling deflection of the top chords occurs in the roof plane.

Material constants $E_l = E_{0,mean}/\gamma_m = (11\ 000/1.3) = 8462$ MPa, $G_{lr} = G_{lt} = E_l/16 = 529$ MPa were adopted from Kessel [10] where E_l is the longitudinal modulus of elasticity and G is the shear modulus. The index l,r,t represents longitudinal, radial and tangential material directions for the wood material. The longitudinal fibre direction corresponds to the length direction of each beam element in the roof structure. The directions r and t also represent the directions of the principle axes of the cross section of the beams elements.

The top chords have a cross section dimensions 60·200 mm, the bottom chord 60·160 mm, the diagonals 60·80 mm, the bracing truss members 60·160 mm and the roof battens 60·40 mm.

Nails with a diameter $d = 3.1$ mm are used to connect the roof battens to the top chords and to each of the flanges of the bracing truss. All the nail joints are simulated with spring elements as shown in Fig. 4. According to Kessel [10] the slip modulus (spring stiffness for shear action in the joint) for this fastener dimension is given as:

$$K_{ser} = \frac{\rho_k^{1.5}\cdot d^{0.8}}{25} = \frac{350^{1.5}\cdot 3.1^{0.8}}{25} = 0.64\ \frac{\text{kN}}{\text{mm}} \tag{11}$$

where K_{ser} is the slip modulus for a wood-to-wood nail joint and ρ_k is characteristic density of the timber material of strength class C24.

The global roof stability is also secured by diagonal wind-stripes acting in pure tension and connecting the roof ridge to the heel supports. The flanges of the bracing trusses are not connected to the adjacent top chords of the trusses (see Fig. 4). The support conditions of each truss in the roof structure are assumed to be simply supported. The static load applied on each truss represents snow and dead loads acting on the top chords and only dead load on the bottom chords, see Fig. 5.

$$q_{top} = a_t\cdot(\gamma_Q\cdot s_k\cdot cos(\alpha) + \gamma_G\cdot g_{k,1}) = 1\cdot(1.5\cdot 0.65\cdot cos(20) + 1.35\cdot 0.68) = 1.83\ \frac{\text{kN}}{\text{m}} \tag{12}$$

$$q_{bottom} = a_t\cdot(\gamma_G\cdot g_{k,2}) = 1\cdot(1.35\cdot 0.60) = 0.81\ \frac{\text{kN}}{\text{m}} \tag{13}$$

where a_t represents the distance between the roof trusses, γ_Q is the partial factor for variable actions, s_k is the characteristic value of snow load, α is the roof slope, γ_G is the partial factor for permanent actions, g_k is the characteristic value of dead load.

Although all of the trusses in Fig. 3 are loaded in the same way, see Fig. 5, the maximum of the lateral displacement of chords occurs in the mid zone of the roof. In Fig. 3, the maximum displacement in the close vicinity of the bracing trusses is about 20% lower than the maximum displacement in the top chords located in the mid zone of the roof. This is possibly because the roof battens do not provide as stiff elastic spring supports to the top chords in the mid-zone as for the other trusses, which are closer to the bracing trusses. The analytical expressions described in the following subsection also support this.

2.2. Analytical methods

The analytical expression for the out-of-plane elastic stiffness of the spring support may be calculated as [4]:

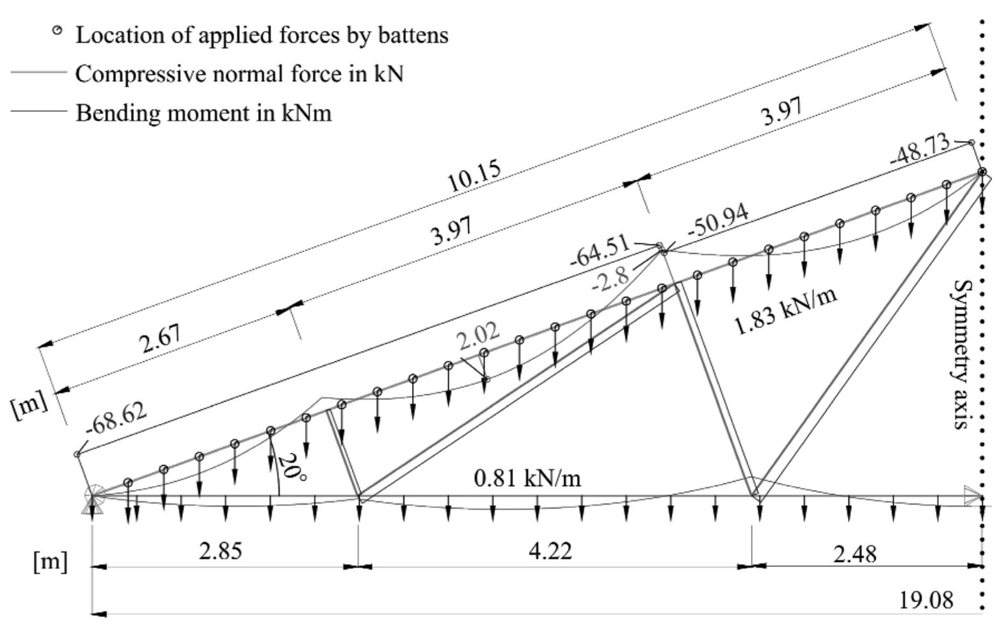

Fig. 5. Variation of normal forces and bending moments in the truss when loaded with a symmetric snow and dead loads.

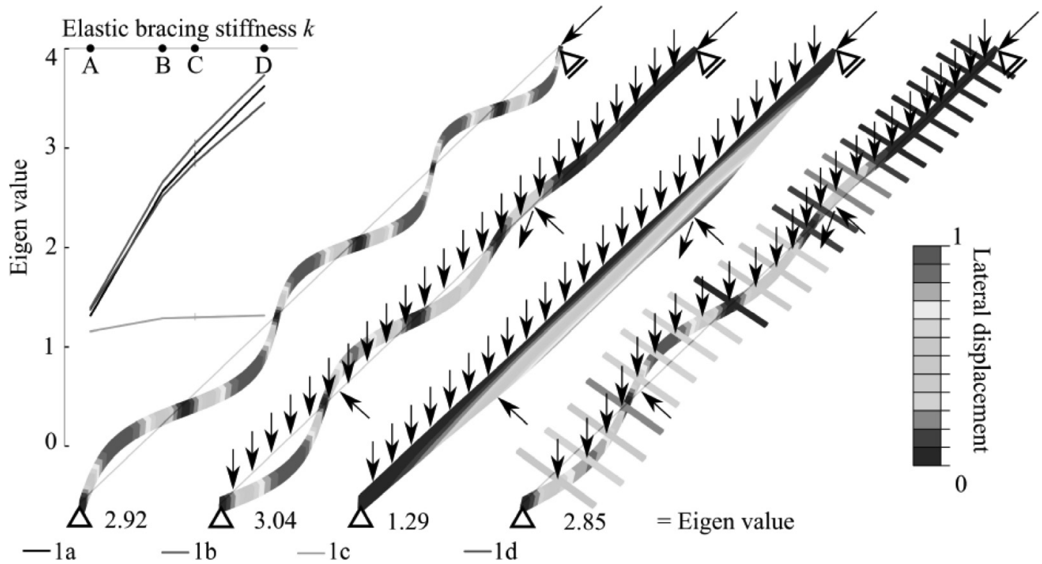

Fig. 6. Influence of out-of-plane bracing stiffness (A, B, C, D in Table 1) on eigenvalues and illustration of buckling modes for four top chord models defined in Table 2. The horizontal elastic bracing is not plotted in the figure.

$$k_s = \frac{1}{\frac{1}{k_{s1}} + \frac{1}{k_{s2}} + \frac{1}{k_{s3}}} \tag{14}$$

where k_{s1} is a (slip) stiffness of the joint between a roof batten and a top chord, k_{s2} is a (slip) stiffness of the joint between a roof batten and the bracing truss and k_{s3} is an effective axial stiffness of one roof batten. The overall bending stiffness of the bracing truss is not included in Eq. (14), since it is assumed to work as a stiff support in the design procedure dealing with the out-of-plane effects in the top chords. The stiffness values in Eq. (14) are calculated as:

$$k_{s1} = \frac{2}{3}\frac{K_{ser}}{\gamma_m}n_1 \tag{15}$$

$$k_{s2} = \frac{2}{3}\frac{K_{ser}}{\gamma_m}\frac{n_2}{n_{btr}} \tag{16}$$

$$k_{s3} = \frac{E_{0,mean}}{\gamma_m}\frac{A_b}{l_{b,ef}} \tag{17}$$

where K_{ser} is the slip modulus for a wood-to-wood single nail joint, γ_m is the partial coefficient for the timber joints, the constant 2/3 in Eqs. (15) and (16) is used to obtain a corresponding ultimate slip modulus, n_1 is the number of nails used for the joint between a roof batten and a top chord, n_2 is the total number of nails used for the joints between a selected roof batten and all the bracing trusses, n_{btr} is the number of braced trusses that this specific batten is connected to, $E_{0,mean}$ is the mean modulus of elasticity for the roof battens, A_b is the cross section area of the roof batten and $l_{b,ef}$ is an effective length of one roof batten for a specific bracing truss used to calculate the effective equivalent axial stiffness of the roof batten. This is given by

$$l_{b,ef} = \frac{n_t(n_t+1)a_t}{2} \tag{18}$$

where n_t equals to the number of trusses between the studied truss and the bracing truss (i.e. 5 for the worst case of structure shown in Fig. 3) and a_t is the c-c distance between the trusses. More explanations and examples of parameters used in Eqs. (14)–(18) are given in Section 2.4.

2.3. Design of the roof members

Because the maximal lateral displacement in Fig. 3 is in the top chord of the truss, the eigenvalue of that mode is used to find the critical normal stress, which in turn is used to calculate the relative slenderness ratio for the top chord as:

$$\sqrt{\frac{f_{c,0,k}}{\alpha_{k,z}\cdot\sigma_{c,k}}} = \sqrt{\frac{f_{c,0,k}}{\sigma_{c,cr,k}}} = \lambda_{rel,z} = \sqrt{\frac{f_{c,0,k}}{\frac{N_{cr,k}}{A_{beam}}}} \tag{19}$$

where $f_{c,0,k}$ is the characteristic compression strength in the wood fibre direction, $\sigma_{c,cr,k}$ is the critical compression stress based on the characteristic load combination, $\alpha_{k,z}$ is the first eigenvalue for the characteristic loads and $\sigma_{c,k}$ is the corresponding characteristic compression stress at a location suitable to calculate $\lambda_{rel,z}$, i.e. the relative slenderness ratio for the top chord.

For columns with varying compression stress (as in this case), the chosen stress could be the average stress over the half wave with the largest out-of-plane deflection or just the stress where the maximum out-of-plane displacement occurs.

Based on the relative slenderness ratio $\lambda_{rel,z}$ in Eq. (19) the effective buckling length can be calculated as

$$l_{eff,z} = \frac{\lambda_{rel,z}\cdot i_z\cdot\pi}{\sqrt{\frac{f_{c,0,k}}{E_{0,k}}}} \tag{20}$$

where i_z is the radius of gyration for the weak axis of the cross section.

The buckling length $l_{eff,z}$ represents a length of a simple supported column (without lateral elastic supports) with the same cross section and the same critical normal force. Hence, it may be used as an input to the software packages ([16,17]), commonly used by the truss designers in the industry.

The displacement field from the buckling analysis shown in Fig. 3 may also be used as an input for the non-linear stress analysis to calculate the stabilising forces in the battens. These stabilising forces, together with the forces induced by the initial inclination of the roof trusses and any external horizontal force component, may be used to design the bracing trusses in the roof plane.

2.4. Parametric study

A number of parametric studies were performed at three geometrical levels; for the top chord, see Fig. 6, for a single truss, see Fig. 5, and for the whole roof model, see Fig. 3. These studies were performed to examine the influence of various variables and simplifications on the simulation results. The stability analysis results can be compared through their eigenvalues because all the simulations relate to the same

Table 1
Stiffness parameters used for four various elastic bracing supports used in the parametric studies, the stiffness symbols "*k*" correspond to Eqs. (14) and (1).

Case	k_{s1} [N/mm]	k_{s2} [N/mm]	k_{s3} [N/mm]	k_s [N/mm]	k [kN/m^2]
A	166.03	33.21	1354.85	27.12	66.80
B	664.12	132.82	1354.85	102.32	252.02
C	664.12	196.19	1354.85	136.21	335.50
D	1328.24	392.39	1354.85	208.64	513.89

roof loaded by a combination of dead and snow load which is also analysed analytically by Kessel, see [10]. The load case is showed in Fig. 5. In Fig. 3, the roof model is simplified compared to the roof analysed by Kessel in [10] to 20 roof trusses braced by two bracing trusses. Two nails are assumed to connect the roof battens to the top chords and to each of the flanges of the bracing truss. This assumption gives the input parameters $n_1 = 2$, $n_2 = 8$ and $n_{btr} = 20$ in Eqs. (15) and (16). The roof analysed by Kessel in [10] consists of 40 roof trusses braced by four bracing trusses which leads to the same values $k_{s,1} = 664.12$ N/mm and $k_{s,2} = 132.82$ N/mm as for the studied roof. The c-c distance between the trusses $a_t = 1$ m and the length $l_{b,ef} = 5(5+1)1/2 = 15$ m is also the same as in the roof analysed in [10]. Therefore, the results of this parametric study may be compared to the conclusions presented in [10].

Table 1 shows four various data sets (referred to as A, B, C, D) for the elastic bracing foundation stiffness used in the parametric studies.

The stiffness combinations in Table 1 are based on the conclusions of Burdzik and Dekker [6], Ormarsson [4], Kessel [10] and a theoretical case with high spring stiffness between the flanges of bracing trusses and the top chords, i.e.:

A Is a "pessimistic" case according to [6], where the slip modulus of each nail is reduced to 25 % compared to the example presented in [10]. These nails are used to connect the roof battens to the top chords and to the bracing trusses, i.e. in eccentric connections (see Fig. 1).

B Is a "numerical" case based on [4], where the spring stiffness of the battens is calculated according to Eq. (14). In this case, all the wood members are assumed to be perfectly straight.

C Is an "analytical" case based on [10], where k_{s2} in Eqs. (14) and (16) is increased by the coefficient $k_{sim} = (1/0.677)$ to consider the influence of the geometrical imperfections of the truss members, according to [10].

D Is an "optimistic" case where the stiffness of the elastic bracing system is increased by assuming the stabilising effect of the contact between the flanges of the bracing truss and adjacent top chords, see Fig. 4.

3. Results and discussion

In Figs. 6, 7 and 9, the influence of the four stiffness combinations in Table 1 (horizontal axes of the plots) on the eigenvalues will be shown for each of the cases: the top chord model, the timber truss model and the 3D roof model. Each eigenvalue from the different models will be plotted against the spring stiffness used to calculate the batten stiffness k_s in Table 1. In all the models, each connection in the bracing truss stabilises five roof trusses, which is based on an assumption used in [10,4]. In the whole roof model, 20 roof trusses are stabilised by 4 connections to the bracing trusses. Connections between the top chords and battens are modelled through springs with the stiffness k_{s1} and connections between battens and flanges of the bracing trusses are modelled through springs with the stiffness equal to $k_{s2}/4$. The cross-section and the modulus of elasticity of beam elements representing the battens are, in accordance with the Eq. (17), comparable to the value of k_{s3} in Table 1. These simulations at different scales provide an opportunity to compare results from the whole roof model with the top chord model and the timber truss model. To study how buckling modes can be influenced by different load variation and boundary conditions Figs. 6, 7 and 9 illustrate various load/boundary cases called 1a-1d, 2a-2d and 3a-3b which are described in Table 2.

3.1. Study of the top chord

To find the out-of-plane buckling length for a typical top chord in the studied truss structure, one top chord was simulated with four different combinations of boundary conditions and external loads. This simplification of the roof structure does not consider buckling of any other structural element than the top chord.

The results in Fig. 6 show variation in the eigenvalue as a function of varying foundation stiffness k_s, for four different sets of loading conditions. The presented buckling modes and the numerically given eigenvalues refer to the lateral spring stiffness data set "C"; it is therefore possible to compare them to the analytical solution in Fig. 2. A comparison of the critical normal force $N_{cr,min}$ calculated with Eq. (7), $N_{cr,min} = 201.8$ kN, and the simulated one in case "1a" indicates good agreement, i.e. $N_{cr} = 2.92 \cdot 68.6 = 200.3$ kN.

In case "1b", the top chord is modelled as a beam on an elastic foundation loaded by forces that represent the internal force distribution shown in Fig. 5. The eigenvalue in "1b" increases slightly compared to "1a", i.e. this approach predicts a more stable structure, i.e. $N_{cr} = 3.04 \cdot 68.6 = 208.5$ kN.

In case "1c", the external axial loads transferred through roof battens are applied to the top edge of the top chord by use of a rigid beam element in between the centerline and the top edge as shown in Fig. 8 and marked in Table 2. The elastic bracing springs are also located at the top edge of the top chord. These load and boundary conditions are causing dominant lateral-torsional buckling which results in much lower eigenvalues than for the other cases. The figure show clear local lateral-torsional buckling shape of the bottom edge. This occurs because the bottom side of the top chord is not braced at all for lateral movement. The stiffening of the elastic bracing system above 250 kN/m^2 does not either improve its stability. Note also that the eigenvalue obtained by this buckling analysis can not be used directly to calculate the buckling length for the top chord. In case "1d", 1.0 meter long beam elements representing battens and 0.12 meter long beam elements representing nails are added to the top chord model. The beam elements representing nails connect beam elements representing battens which do not intersect the beam element representing the top chord. Mechanical properties like the modulus of elasticity and the cross-section were chosen according to Burdzik [6] to represent the slip modulus of each simulated nailed connection between the batten and the top chord. Compared to the case "1c", the increased torsional stiffness because of the nailed roof battens is resulting in the buckling mode with a higher eigenvalue and dominant lateral buckling. However, the eigenvalue is still lower than in case "1b".

The results show clearly how the top chord model is sensitive for external axial loads and external location of the lateral bracing members. To study this stability phenomenon in more detail, single truss models (type "double-W truss") were created.

3.2. Study of a single truss

The results from the study of the single truss are illustrated in Fig. 7. The buckling modes shown in Fig. 7 for the trusses are related to the spring stiffness data set "C" in Table 1. It is therefore possible to compare them with an analytic modes in Fig. 2 and with simulated modes in Fig. 6.

In case "2a", the single truss model is loaded with line-loads (see Fig. 5) assigned to the centre-lines of the chords. The roof battens are modelled with lateral springs located at the centre-lines of the top chords. The connections between chords and diagonal members and the

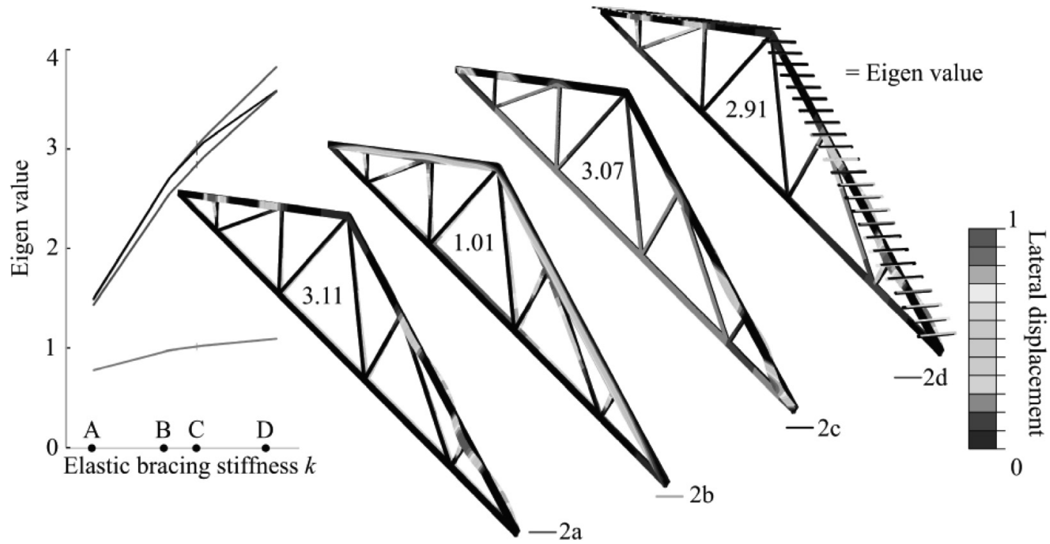

Fig. 7. Influence of out-of-plane bracing stiffness (A, B, C, D in Table 1) on eigenvalues and illustration of buckling modes for four single truss models defined in Table 2. The horizontal elastic bracing is not plotted in the figure.

Table 2
Description of boundary cases used in Figs. 6, 7 and 9. Bullet points mark cases where are used rigid beam elements (see Fig. 8), blank boxes point out cases following static sketch in Fig. 5.

Model name	Stiffness case	Rigid beams	Model description
1a	C		Top chord, constant axial load
1b	C		Top chord, non-uniform internal force distr.
1c	C	•	Top chord, lateral-torsional buckling
1d	C		Top chord, battens and nails
2a	C		Truss, loads and lateral springs to centre-lines
2b	C	•	Truss, pinned joints, lateral-torsional buckling
2c	C	•	Truss, stiff joints
2d	C		Truss, battens and nails
3a	C		3D roof, stiff bracing truss
3b	C		3D roof, weak bracing truss

connections between chords in the crown and heels of the truss are modelled by six rigid constraints (three for translations and three for rotations). According to [18], such a model should provide reasonably accurate results compared to the real behaviour (within approximately 10 per cent). This truss model brings a higher eigenvalue than the single top chord model "1a" due to the stabilising effect of a more correct stiffness of the heel joint, crown joint and the jointed diagonals to the top chord.

In case "2b", all joints are modelled as pinned joints and the battens are modelled as a lateral elastic springs located at the top edges of the top chords as it is shown in Fig. 8. The line-load representing the snow and dead loads is also applied to the top edges of top chords. This truss model gives a lower eigenvalue than the single top chord model "1c", i.e. due to the lateral-torsional instability of the whole truss.

Case "2c" differ from case "2b" because of the large rotational stiffness between the truss members. The slight difference in the eigenvalue between case "2c" and "2a" is due to the influence of the lateral torsional buckling of the top chords. The battens are modelled as

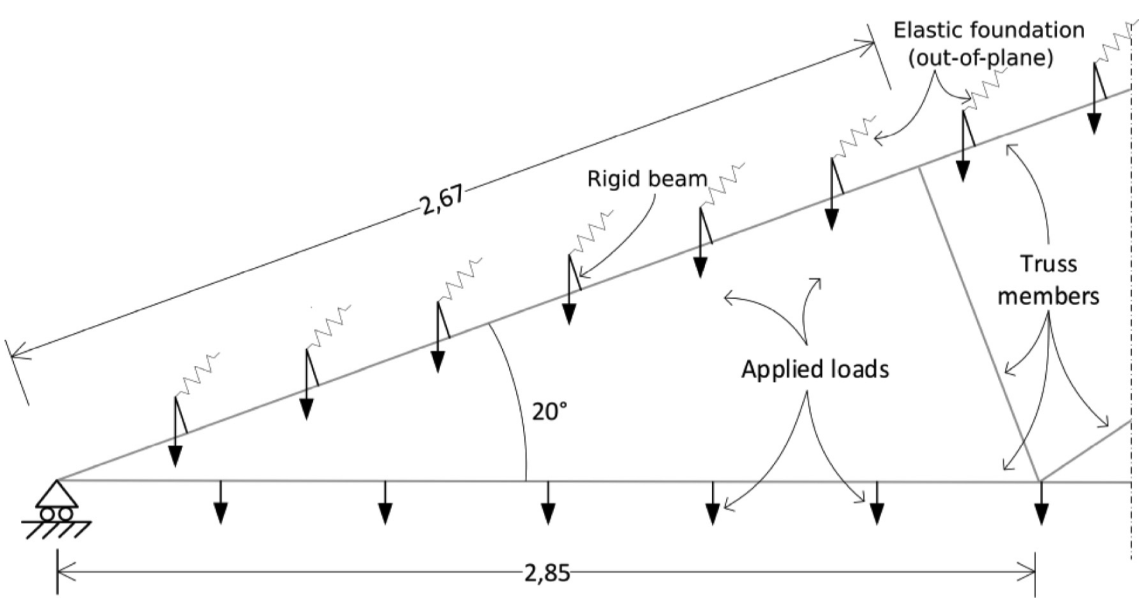

Fig. 8. Visualisation of the rigid beams between the centerline and the top edge of the top chord used to create external location of the axial loading and the bracing supports.

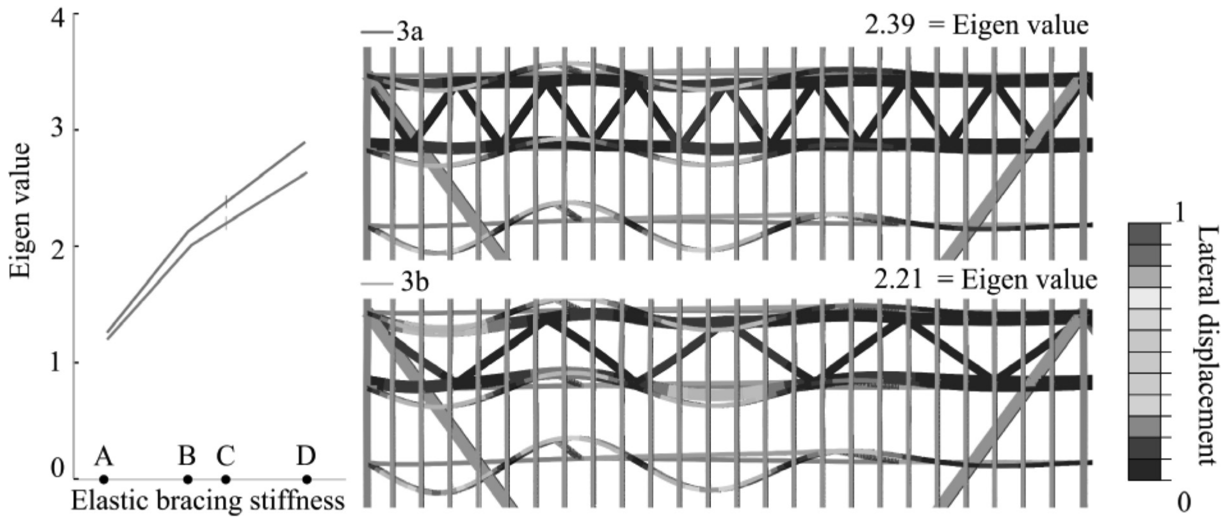

Fig. 9. Influence of out-of-plane bracing stiffness (A, B, C, D in Table 1) on eigenvalues and illustration of buckling modes for two 3D roof models defined in Table 2.

described in the case "2b".

In case "2d", beam elements representing battens are added to the case "2c". The battens are connected by beam elements representing nails to the top chords which is increasing lateral-torsional stability. The snow and dead load is applied to the battens instead of to the top chords. Here, the eigenvalue is lower than in the most simple case "2a", due to the effect of the eccentric acting of the load to the top chords.

In summary, the possibility of lateral-torsional buckling of both, the top chord and the whole truss significantly affects the eigenvalue of the studied single truss models.

3.3. Study of the whole roof

To study how bracing truss stiffness influences the total stiffness of the lateral bracing system, two 3D models of the entire roof structure were created. In both roof models the eccentricity between the centrelines of the roof battens and the top chords is neglected.

Since the presented buckling modes in Fig. 9 of the trussed roof structures are related to the spring stiffness data set "C" in Table 1, it is possible to compare them to buckling results in Figs. 2, 6 (case "1b") and Fig. 7 (case "2a").

The roof structure in case "3a" uses stiffer bracing truss than the roof structure in case "3b", resulting in slightly different eigenvalues for the structures. This is less significant when the spring stiffness of the connections between battens and trusses is changed (data sets C and D). When the stiffness of the batten-top chord connection is highest, the compliance in the bracing truss affects the eigenvalue the most. In the magnified buckling mode in Fig. 9, the top chords of the bracing trusses have significantly different shape than the adjacent flanges of the bracing trusses. As in the technical solution shown in Fig. 4 where no connectors are between the flanges of the bracing trusses and the adjacent top chords, this allows small deformations between them. The displacement field in the bracing truss shows that a bracing system modelled by beam elements in its entirety acts weaker than in the simplified version using springs with analytically calculated stiffness. When comparing cases "1b", "2a" and "3 a-b", the simulations of the whole roof structure gives noticeably lower eigenvalues. This indicates that bracing truss stiffness is an important parameter that affects the lateral stability of the top chords of the studied roof structure. An efficient contributor to the overall roof stability seems to be stiffening up the nail connections between the roof battens and flanges of the bracing trusses.

3.4. Design of roof battens

To calculate the design forces acting in the bracing system a geometric nonlinear analysis of the timber truss is utilised. The initial imperfection used for the timber truss is based on the out-of-plane buckling mode "2a" shown in Fig. 7.

In the nonlinear stress analysis used to generate the spring force variation in Fig. 10, the maximum initial bending eccentricity of the largest half-wave is set to 1/300 of its length which corresponds to 6.8 mm. The timber truss is loaded incrementally up to the design load shown in Fig. 5. Fig. 10 shows the variation in spring forces along the top chord at this load state. The maximum spring force $F_d = 371$ N occurs in the third half wave from the eaves. This value is considerably smaller compared to the design force value calculated according to EC5 [19] using the maximal design force from Fig. 5 as

$$F_{d,EC5} = \frac{N_d}{50} = \frac{68.6}{50} = 1.37\ \text{kN} \tag{21}$$

The difference between calculated and simulated values is partly explained with the small initial imperfection value used in the model and because the Eq. (21) is based on a buckling mode with half-waves of the same length as the c-c distance between the roof battens. The results of the buckling analyses shown in Figs. 6, 7 and 9 indicate that

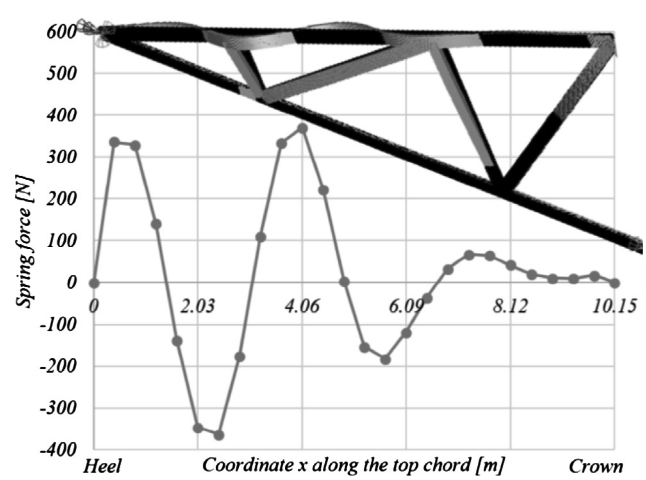

Fig. 10. Variation in lateral bracing forces (spring forces) along the top chord based on geometric nonlinear stress analysis of a single timber truss loaded with a design load in Fig. 5 together with illustration of the initial geometrical imperfection shape of the truss.

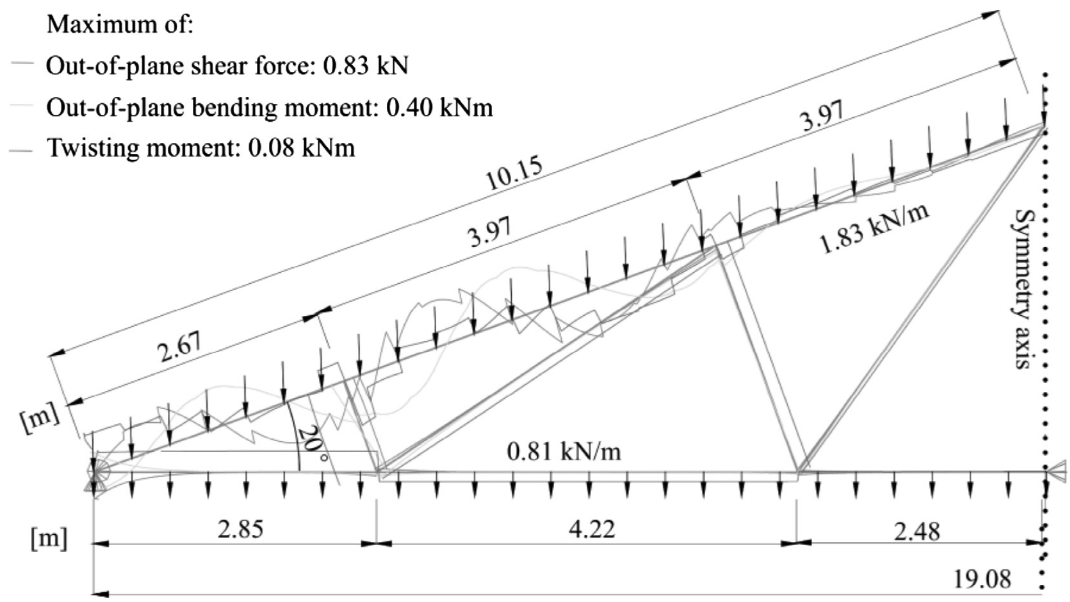

Fig. 11. Variation of twisting moment, out-of-plane shear and out-of-plane bending moment simulated with geometric nonlinear stress analysis of the truss "2a".

this assumed buckling mode in practice never occurs for the timber truss studied, i.e. the EC5 [19] expression significantly overestimates the design force in the connections and underestimates the buckling length in the top chord.

The design force F_d is used to design the roof battens and the nail connections between the roof battens and the timber trusses. The geometrical imperfections in the out-of-plane direction of the top chord may also indicate non-negligible out-of-plane forces acting on the truss (see Fig. 11).

The internal force and moment diagrams in Fig. 11 indicate that nonlinear stress analysis can also be used to calculate twisting moment, out-of-plane shear and the out-of-plane bending moment in the studied truss. These three force components are neglected in commonly used in-plane truss design. In relation to the cross-sectional characteristics of the analysed top chords, the out-of-plane bending is the most critical. It causes a maximal bending stress of magnitude $\sigma_{m,z} = 3.3$ MPa which is about 20 % of the design load-bearing capacity of the analysed top chord. The internal forces in Fig. 11 are also contributing to increased loading on the connections when designing the truss. However, for punched metal plate fasteners, which are commonly used connectors in pitched long-span timber trusses, the design procedure does not include the out-of-plane behaviour of the joints. Therefore, their different out-of-plane load carrying capacities are still unknown.

3.5. Design of the bracing truss

Another possible use of the results from the geometrical nonlinear stress analysis is for bracing truss design. A bracing truss should transfer forces caused by wind loads acting on the gable of the building and lateral stability forces from the top chord of the timber trusses to the bracing system of the walls. A bracing truss is typically designed to stabilise about 8 to 10 trusses. Design of the bracing structure is based on a load combination (wind- snow- and dead load), where the wind load is treated as a dominating load and the corresponding (upward) wind load acting on the roof is neglected since it is the favourable load in this load combination. The wind load on gable is only partly carried by the bracing truss. For the adopted load combination the design wind pressure acting on the gable is $q_{wp,d} = 0.77\,\text{kN/m}^2$. The part of the pressure supported by the bracing truss can be expressed as a linear line load $q_{w,d}$ with maximal value 1.33 kN/m in the ridge of the roof.

To design the bracing truss, two types of initial imperfections are imposed. The first one is that the top chord has a bow imperfection with eccentricity $e = l_{bt}/300 = 0.033$ m and the next one that the slope of the truss out of its plane is $\phi = 0.02(2.5/h_{tr})(180/\pi) = 0.83°$. These imperfections are used for the nonlinear stress analysis. To create this initial geometry a buckling analysis of a truss with an initial slope of $\phi = 0.83°$ and without springs representing battens is performed. In the geometric nonlinear analysis, the truss is loaded incrementally up to the design load shown in Fig. 5. A variation in the lateral bracing forces along the top chord is presented in Fig. 12.

Fig. 12 shows the variation of the lateral bracing force along the top chord with 10 times magnified initial bow imperfection and 1000 times magnified vectors showing the out-of-plane displacements (in colours) of the top chord after the applied design load. The distribution of stabilising forces shows a noticeable trend to follow the critical buckling shape influenced by positions of jointed truss diagonals to the top chord. The distribution also shows that the most loaded connections between the battens and the flange of the bracing truss might not defined by the maximal magnitude of the wind load, as according to the assumption of uniformly distributed stabilising forces in EC5.

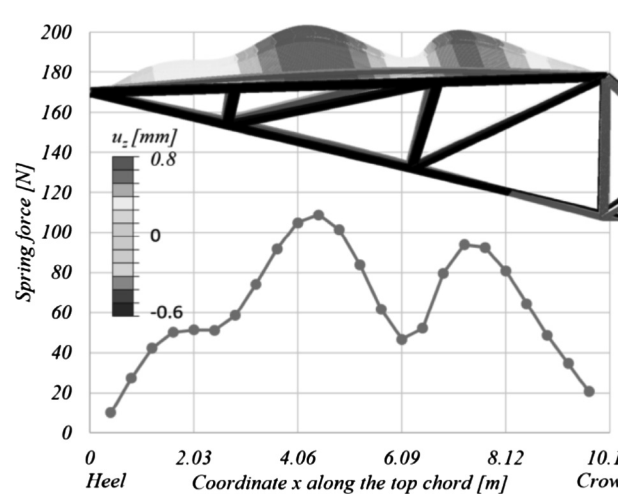

Fig. 12. Variation in lateral bracing forces (spring forces) along the top chord calculated with the nonlinear stress analysis and illustration of the initial bow imperfection and the out-of-plane deformation caused by the design load shown in see Fig. 5.

4. Summary of the found results

Three parametric studies were performed with the finite element software Abaqus® to study how different spring stiffness influences the out-of-plane stability behaviour of the trussed timber roof structure, see Fig. 1.

The first study was a beam on an elastic foundation, representing the simplified model of a top chord braced with a semi-rigid bracing system of roof battens. The stiffness of the battens was derived by using an analytical expression under the assumption of negligible deflections in the bracing trusses. Based on these results, conclusions on how much the top chord is stabilised by battens can be drawn, assuming that the heel joint and ridge joint act as pinned supports for the beam. The model results were used to compare the analytical and the numerical results, see Eq. (1). Both models give the same number of half-waves for the critical buckling mode, resulting in good agreement of the critical buckling forces and the buckling lengths.

The second study was made on a single timber truss, where the top chord was braced by lateral elastic springs representing the roof battens. This model considers the variation of the internal normal forces along the top chord of the pitched truss structure, see Fig. 5. This variation causes the maximum out-of-plane buckling of the top chord to occur close to the heel of the truss. The single truss model could also better consider the jointed elements influence on the buckling results in more sophisticated way than the individual top chord model. In this study, two types of joints (pinned and constrained) were used to connect the chords and the diagonal members. The truss with constrained connections was also analysed with a geometric nonlinear stress analysis, using initial imperfections from the buckling analysis. The model showed non-negligible out-of-plane forces acting on the truss connections. However, all these out-of-plane forces are neglected in commonly used two-dimensional truss design, which potentially could cause under designed connections in the truss structures. To improve this knowledge, the out-of-plane stiffness and capacity of punched metal plate connections is a scope for future research using advanced (shell/solid element based) numerical simulations in combination with experimental testing.

The third study was performed on an entire roof structure using a 3D spring/beam model. The model was implemented to load the complex bracing system and there achieve stiffness values used in analytical and more simplified models. The deflection of the bracing truss contributed to the fact that the global stiffness was significantly smaller than those values calculated analytically.

5. Conclusions

The presented analytical and numerical analysis can be used to calculate more realistic out-of-plane buckling lengths than those typically used in truss design today. The entire roof buckling analysis indicates that the stiffness of the bracing truss is an important parameter that affects the lateral stability (in term of the out-of-plane buckling lengths) of the top chords in the analysed roof structure.

The buckling analysis of the single truss and individual top chord models, specifically the eccentricity between the centrelines of top chords and battens, clearly shows that lateral torsional buckling of the top chord negatively influences the load carrying capacity for the out-of-plane buckling failure. This could be a critical for some connections especially if they are not properly designed.

The eigenvalue of the modelled long-span pitched roof structure, based on realistic dimensions of used timber boards, is close to three which is a typical value for this type of structure. For values lower than so a more accurate second order analysis should be applied [16].

Based on the geometric nonlinear analysis it can be concluded that out-of-plane forces caused by the top chord members may occur for long-span pitched timber trusses. These out-of-plane stability forces are especially important for connection designs of the nail joints between the roof battens and top chords and for the punched metal plate connections between chords and diagonal members. The design of these connections regarding both in-plane and out-of-plane loading is a scope for further studies. Another scope for further studies is the experimental verification of the presented simulations to improve the current state when only the analytical approach presented by Kessel [10] is used for comparing the results of various numerical analyses.

Declaration of Competing Interest

None declared.

Acknowledgement

This work has been supported by the Ministry of Culture of the Czech Republic, research grant NAKI II DG18P02OVV012 - Sustainable Management of Historical Buildings.

References

[1] Frese M, Blaß HJ. Statistics of damages to timber structures in Germany. Eng Struct 2011;33(11):2969–77.
[2] Šilih S, Premrov M, Kravanja S. Optimum design of plane timber trusses considering joint flexibility. Eng Struct 2005;27(1):145–54.
[3] Klasson A. Slender roof structures: Bracing, modelling, full-scale testing and safety [Ph.D. thesis]. Faculty of Engineering, LTH, defence details Date: 2018–12-10 Time: 09:00 Place: Lecture hall MA3, Mathematics Annex building, Sölvegatan 20, Lund University, Faculty of Engineering LTH. External reviewer(s) Name: Doudak, Ghasan Title: Associate Professor Affiliation: University of Ottawa, Canada; 2018.
[4] Ormarsson S, Vessby J, Källsner B, Filchev I. Numerical analysis of failure modes and force distribution in a pitched roof structure of wood. WCTE 2016 world conference on timber engineering, August 22–25, 2016, Vienna, Austria. 2016.
[5] Maraghechi K, Itani RY. Influence of truss plate connectors on the analysis of light frame structures. Wood Fiber Sci 2007;16(3):306–22.
[6] Burdzik W, Dekker N. A rational approach to predicting the buckling length of compression chords in prefabricated timber truss roof structures braced by means of diagonal bracing. J South Afr Inst Civ Eng 2012;54(1):81–9.
[7] Stanway G, Chapman J, Dowling P, Curtin W. A simply supported imperfect column with a transverse elastic restraint at any position. Part 1: Behaviour. (winner of 1993 bill curtin medal). Proc Inst Civ Eng Struct Build 1992;94(2):205–16.
[8] Song X, Lam F. Laterally braced wood beam-columns subjected to biaxial eccentric loading. Comput Struct 2009;87(17–18):1058–66. https://doi.org/10.1061/41016(314)54.
[9] Pienaar F. The effective length and bracing requirements for out of plane buckling of timber rafters in compression. S Afr For J 1986;137(1):13–25. https://doi.org/10.1080/00382167.1986.9629639.
[10] Kessel MH, Kühl A. Aussteifung von Nagelplattenkonstruktionen (Bracing of Top Chords by means of Roof Battens). Fraunhofer-IRB-Verlag; 2011.
[11] Timoshenko S, Jere J. Theory of elastic stability; 1961.
[12] Winkler E. Die lehre von der elastizität und festigkeit (the theory of elasticity and stiffness), Dominicus, Prague.
[13] Euler L. de altitudine columnarum sub proprio pondere corruentium. Acta Acad Sci Petropolitanae 1778;1:163–93.
[14] Theiler M, Frangi A, Steiger R. Strain-based calculation model for centrically and eccentrically loaded timber columns. Eng Struct 2013;56:1103–16.
[15] A.U. Manual, Version 6.16, ABAQUS Inc.
[16] BOVA, FINE, Ukázka návrhu vazníku v programu truss 2d. dřevěné střešní konstrukce - řešení pro výrobce (demonstration of truss design in truss 2d software) — bova-nail; 2006. http://www.bovanail.cz/podpora/truss-2d.php.
[17] GmbH MI. Mitek industries; 2015. http://www.mitek.de/Downloads/RoofConTrussCon/RoofCon-TrussCon/.
[18] Pienaar F. The influence of various factors on the accuracy of the structural analysis of timber roof trusses, Proceedings of CIB subject group W18, Karlsruhe (15–14-2).
[19] B. EN, 1-1. eurocode 5: Design of timber structures, General. Common rules and rules for buildings, BSI.